Lasers in Eng., Vol. 17, pp. 59–73
Reprints available directly from the publisher
Photocopying permitted by license only

Laser Surface Treatment of Ti-6Al-4V for Bio-Implant Application

A. BISWAS[1], L. LI[3], T. K. MAITY[3], U. K. CHATTERJEE[1], B. L. MORDIKE[4], I. MANNA[1], AND J. DUTTA MAJUMDAR[1*]

[1]*Dept. of Met. & Mat. Engg., I. I. T., Kharagpur, W.B. – 721302, India*
[3]*Dept. of Biotechnology, I. I. T., Kharagpur, W.B. – 721302, India*
[2]*School of Mech., Aero. & Civil Engg., Univ. of Manchester, Manchester-M60, 1QD, UK*
[4]*Instt. Of Maters. Sci. & Technol., T. U. Clausthal, D-38678 Clausthal zellerfeld, Germany*

The present study aims at enhancing the wear resistance of Ti-6Al-4V by laser surface melting and nitriding and subsequently, studying the influence of laser surface treatment on the corrosion resistance in a simulated body fluid and also the bio-compatibility. The laser surface treatment is carried out using a high power continuous wave diode laser with argon and nitrogen as shrouding gas. Laser surface melting leads to an increased volume fraction of acicular martensite and a decreased volume fraction of the β phase in the microstructure. Laser surface nitriding leads to the formation of titanium nitride dendrites. The micro-hardness could be improved up to a maximum of 450 Hv in laser surface melting and 900–950 Hv in the case of laser surface nitriding as compared to 260 Hv of the as-received substrate. Surface melting increases the corrosion potential (E_{corr}) and primary potential for pit formation (E_{pp1}) significantly as compared to the as-received Ti-6Al-4V. However, when processed under similar conditions, surface nitriding shifts E_{corr} marginally in the more noble direction, and increased E_{pp1} as compared to Ti-6Al-4V. The biocompatibility behaviour shows a superior cell viability on surface nitriding and an inferior cell viability on surface melting as compared to the as-received Ti-6Al-4V.

Key words: Ti-6Al-4V, laser, melting, nitriding, wear, corrosion, biocompatibility

*Corresponding Author: E-mail: jyotsna@metal.iitkgp.ernet.in

INTRODUCTION

Titanium and its alloys are widely used as surgical implants because of their good corrosion resistance, high specific strength and biocompatibility [1–3]. However, applications in pure titanium are sometimes limited due to its poor wear resistance. In addition, the loss of adhesion at the interface was found to be caused by the existence of a layer of porous titanium oxide [4]. Over the last decade, various surface modification techniques have been developed to improve the interfacial bonding of the alloy and the bone [5–8]. In order to improve the tribological properties of this metal, nitriding of titanium is commonly applied [9, 10]. TiN used as a hard coating is chemically inert, which in turn provides good corrosion protection. Such a surface layer will also discourage the formation of oxides during subsequent processes. In addition, important surface characteristics which can contribute to a strong interfacial joint are (i) the existence of polar chemical groups or coupling agents on the surfaces to be bonded and (ii) an increased surface roughness, giving rise to an improved mechanical interlocking or increased bondable surface area [11].

The laser, as a source of monochromatic and coherent radiation, has been used for a wide range of applications in materials processing [12]. In the past, laser surface alloying has been used extensively for modification of surface microstructures and/or composition of titanium to improve the wear and high temperature oxidation resistance [13]. Laser surface remelting of titanium in a nitrogen containing environment is popularly known as laser gas nitriding (LGN), which can produce composite nitride surface layers with enhanced surface performance [14–16]. The advantages of laser assisted surface treatment over conventional diffusion aided surface treatment include the ability to deliver a high power/energy density (10^3 to 10^5 W/cm^2), high heating/cooling rate (10^3 to 10^5 K/s) and solidification speeds (1–30 m/s) [12].

Laser gas nitriding of Ti and Ti-6Al-4V (Ti64) alloys has been extensively investigated with the aim of improving the tribological properties [9, 17–20]. A complex microstructure is produced in the solidified melt pool depending on the applied laser power, beam size, specimen displacement rate, beam mode (stationary or spinning) and the nitrogen concentration [21]. Cracking was found to be a critical problem in laser nitriding of titanium alloys due to the large residual compressive stress developed in the nitrided zone [22]. Man *et al*. [23] nitrided the surface of Ti-6Al-4V substrate using a continuous wave Nd:YAG laser and reported a better adhesion between the glass coating and the LGN-etched specimen as compared to the sand blasted specimen [23].

In the present study, laser surface melting and nitriding of a Ti-6Al-4V substrate was carried out using a ‘Laserline’ diode laser. It is relevant to

mention that metallic materials have a higher absorptivity at the wavelength of diode lasers. Laser surface nitriding of Ti-6Al-4V using a diode laser has not been reported elsewhere. The laser parameters have been selected to avoid the formation of micro-cracks in the laser nitrided surface. The effect of laser parameters on the microstructure, phases and micro-hardness has been studied in detail. The aqueous corrosion in a simulated body fluid of the laser nitrided and as-received Ti-6Al-4V has been evaluated. In addition, the bio-compatibility of the nitrided and melted surfaces have been compared with that of as-received Ti-6Al-4V.

EXPERIMENTAL

In the present investigation, Ti-6Al-4V (Ti64) specimens of dimension: 20 mm × 20 mm × 5 mm was chosen as substrate. The substrate surfaces were sand blasted prior to laser processing in order to clean the surface and improve the absorptivity. Laser surface melting and surface nitriding were carried out using a 1.5 kW continuous wave (CW) diode laser with a rectangular beam (3.5 × 2 mm area) and argon and nitrogen as shrouding gas at a gas flow rate of 5 l/min. The specimens were mounted on the CNC controlled X-Y stage which was moved at a speed of 1–5 mm/s. The relative speed between the laser beam and the specimen was maintained constant to ensure the substrate-laser beam interaction time and a larger coverage in area. In order to achieve micro-structural and compositional homogeneity of the laser treated surface, a 25% overlap between the successive melt tracks was maintained. Sufficient time was allowed for each track to cool to room temperature before the treatment was resumed. A large number of trials were undertaken using a wide range of laser powers and scan speed combinations to establish the effect of the laser parameters on the characteristics of the composite layer. The scan speed was maintained constant at 6 mm/s. The detailed investigation on the influence of the process parameters on the characteristics and properties of the melted and nitrided surface have been reported elsewhere [24]. The microstructures of the melted and nitrided layers (both the top surface and the cross section) were characterised by optical and scanning electron microscopy. A detailed analysis of the phases was carried out by X-ray diffractometer. Residual micro-stress and crystallite size were calculated from the peak broadening using the Scherrer formula to deduct the instrumental broadening effect [25]. The micro-hardness of the composite layer, both on the top surface and along the cross sectional plane, was measured by using a Vickers micro-hardness tester using a 25 g applied load. Finally, the pitting corrosion behaviour of the laser composite surfaced specimen was compared with that of the untreated one by calculating the corrosion rate derived from the potentio-dynamic anodic polarization study in Hank's solution with

the following electrolyte composition (g/l): 0.185 $CaCl_2$, 0.4 KCl, 0.06 KH_2PO_4, 0.1 $MgCl_2$, $6H_2O$, 0.1 $MgSO_4.7H_2O$, 8 NaCl, 0.35 $NaHCO_3$, 0.48 Na_2HPO_4 and 1.00 D-glucose. In the corrosion study, a standard calomel electrode (SCE) was used as the reference electrode and platinum was used as the counter electrode [26]. Polarisation was carried out from −2000 to +7000 mV (SCE) at a scan rate of 2 mV/s. The Tafel plot [26] showed the log. of the current density plotted against a function of the voltage. The slope of the Tafel plot in the linear region in the anodic direction is called the anodic Tafel constant and in the cathodic direction is called the cathodic Tafel constant. The corrosion current (i_{corr}) was determined from the intersection of these two linear plots. Subsequently, the pitting corrosion behaviour was determined by measuring the primary potential for pit formation, E_{PP1}, the potential at which there is a sudden rise in the current density for a small increase in potential, and pit growth, E_{PP2}, the potential corresponding to the intersection between the forward and reverse cycle of the polarization curve.

Finally, the biocompatibility behaviour of the treated and as-received samples were studied by measurement of the in-vitro cyto-toxicity and cell proliferation by the MTT [3-(4, 5-dimethyl thiazol-2-yl) 2, 5-diphenyl tetrazolium bromide)-based colorimetric assay described by Mosmann [27]. The MTT assay depends on both the number of cells present and on the mitochondrial activity per cell. The mitochondrial enzyme succinate-dehydrogenase within viable cells is able to cleave the tetrazolium salt MTT into a purple coloured product (formazan) which is soluble in dimethyl sulfoxide (DMSO;Sigma chemical Co) [28]. It is proposed that the amount of formazan produced is proportional to the number of viable cells present [29, 30]. The formazan salt resulting from the reduction of MTT is dissolved in dimethyl- sulfoxide and the absorbance is read at 595 nm using an automatic plate reader (Micro plate reader, BIO RAD, Model 550). The cell viability is extrapolated from the optical density $(OD)_{595}$ values and expressed as percent survival using the following formula: % cell viability=[OD_{595} of surface treated sample/OD_{595} of positive control sample (Petri plate)] × 100.

In the present experiment, the as-received, laser surface melted (lased with a power of 700 W) and lased surface nitrided (lased with a power of 600 W) Ti-6Al-4V were carefully polished and autoclaved. 4 ml of 10^5 cells of L-929 (mouse fibroblast cell line) was transferred to a Petri plate containing the specimen. The plates were incubated in a carbon-dioxide chamber containing 5% CO_2 at 37°C in a humidified chamber for 24 hours [31]. After 72 hours incubation with proper control (polystyrene petriplate), the cell culture was treated with MTT solution and incubated for 4 hours at 37°C. Then the medium was replaced with dimethyl-sulfoxide and absorbance of the solution was measured by a plate reader (Micro plate

reader, BIO RAD, Model 550) at 595 nm. Each experiment was repeated for 3 times and average reading was taken into consideration.

RESULTS AND DISCUSSION

In this section, a detailed characterisation of the microstructure and phases in the laser surface melted and laser surface nitrided Ti-6Al-4V was ascertain the characteristics of the modified layer. In addition, mechanical measurements and the corrosion properties of the surface melted and surface nitrided layers were evaluated and compared with the as-received Ti-6Al-4V. Finally, the biocompatibility behaviour was evaluated by cell proliferation/viability studies. The results of the mechanical and electrochemical properties of the composite layer are discussed in detail.

Characteristics of the melted/nitrided zone

Figure 1 shows the scanning electron micrograph of the top surface of the as received Ti-6Al-4V substrate used in the present study. The microstructure consists of elongated α-Ti and the presence β-Ti lamellae in the inter-granular region. The as-received microstructure showed that it had been cold rolled. The average grain size varied between 15 μm and 25 μm. Figures 2(a, b) show the microstructures of (a) laser surface melted and (b) laser surface nitrided Ti-6Al-4V at a power of 600 W. Laser surface melting led to a significant refinement of the microstructure and due to the

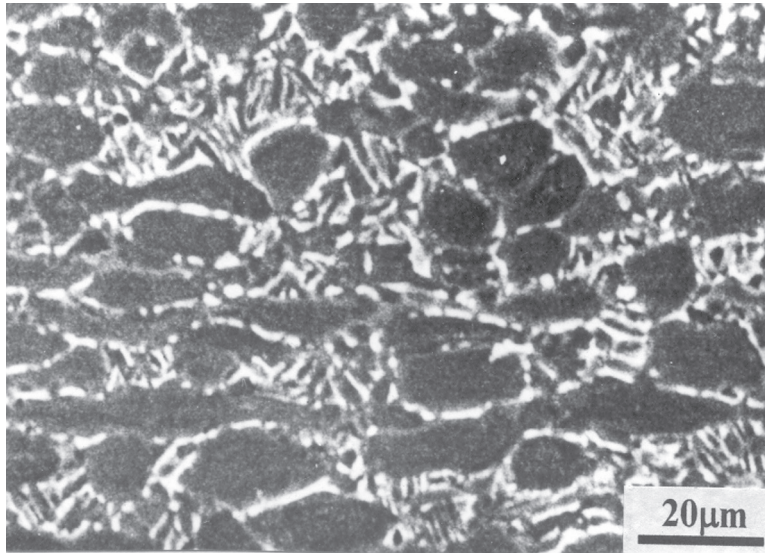

FIGURE 1
Scanning electron micrograph (SEI) of as received Ti-6Al-4V.

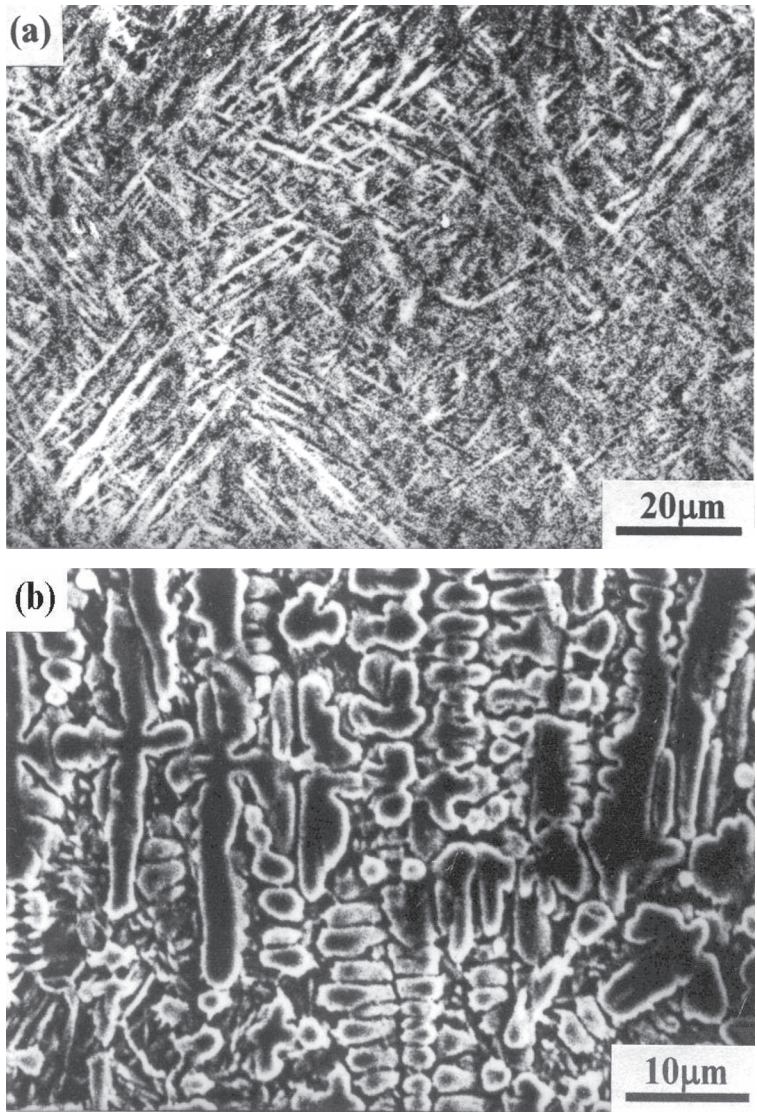

FIGURE 2
Scanning electron micrograph (SEI) of the top surface of (a) laser surface melted and (b) laser surface nitrided Ti-6Al-4V lased with a laser power of 600 W.

very high cooling rate caused acicular α' martensite to form. This fine, acicular martensite has a hexagonal closed packed structure and possesses a high hardness but relatively low ductility and toughness [32]. On the other hand, laser surface nitriding caused titanium nitride (TiN) dendrites to form in an α-Ti matrix. The dendrites were very fine with an average

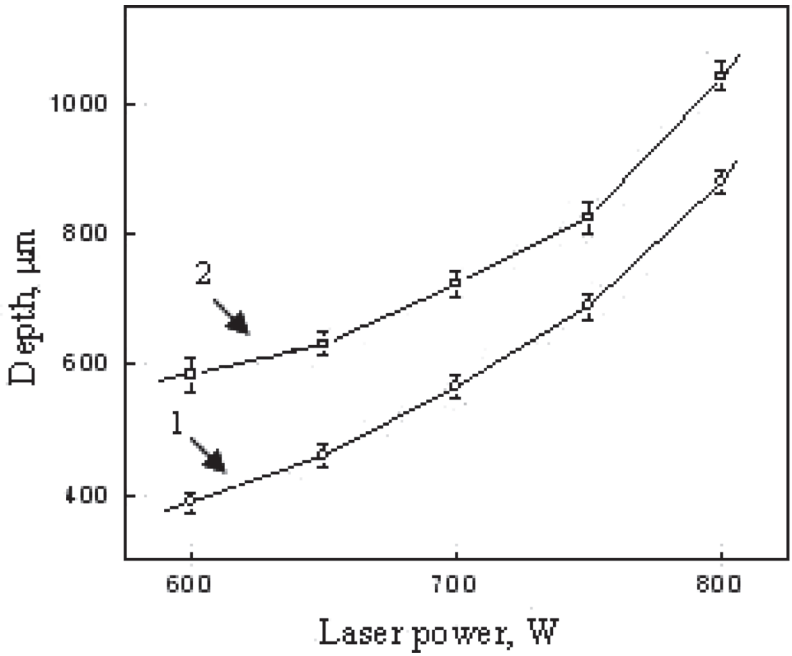

FIGURE 3
Variation of depth of melting (plot 1) and nitriding (plot 2) with applied laser power.

primary arm spacing of 2.5 to 4 μm. A detailed study of the influence of laser parameters on the volume fraction of titanium nitrides has been reported elsewhere [24]. The depth of the melted/nitrided zone determines the lifetime of the component. Figure 3 shows the effect of the applied power on the depth of melting (plot 1) and nitriding (plot 2) for laser surface melted and nitrided Ti-6Al-4V. It was observed that depth of the melting and nitriding increased with increasing power. In addition, molten depth achieved in surface nitriding was higher than that of melting due to the generation of heat during the transformation from α-Ti to TiN [34], which may lead to coarsening of the microstructure.

Figures 4(a–c) show the X-ray diffraction profiles of the surface of (a) as received, (b) laser surface melted (with a power of 600 W) and (c) laser surface nitrided (with a power of 600 W) Ti-6Al-4V. The X-ray diffraction profiles show that the 'as received' Ti-6Al-4V used in the presence study consists of a mixture of α and β-Ti. The relative volume fraction of β-Ti was lower than that of the α-Ti. Laser surface melting reduced the volume fraction of the β phase significantly (cf. Figure 4(b)). Laser surface nitriding on the other hand, led to the formation of titanium nitride, TiN, with the presence of only a few α-Ti peaks. Table 1 shows the summary of the results of the X-ray diffraction study of laser surface melted and

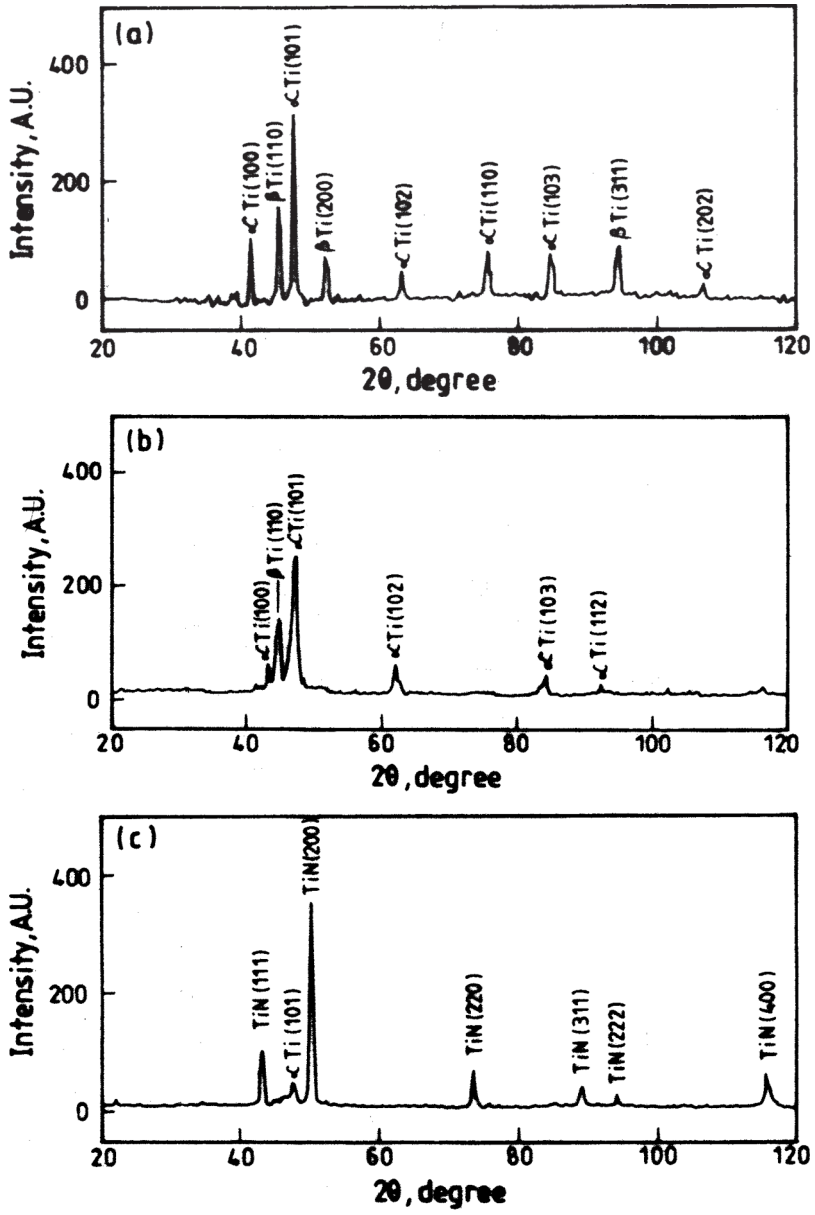

FIGURE 4
X-ray diffraction profile of (a) As received, (b) laser surface melted (with a power of 600 W) and (c) laser surface nitrided (with a power 600 W) Ti-6Al-4V.

TABLE 1
Volume percentage of phases and lattice strain of as received, surface melted and surface nitrided of Ti-6Al-4V calculated from X-ray diffraction analysis.

Sl. No.	Specimen history	Phases and volume %	Lattice strain (%)
1	As received Ti-6Al-4V	αTi, 70	0 %
		βTi, 30	-
2	Melted Ti-6Al-4V	αTi, 80	0.577
		βTi, 20	0.573
3	Nitrided Ti-6Al-V	αTi, 6	0.639
		TiN, 94	-

laser surface nitrided Ti-6Al-4V. The decrease in the β-Ti content from 30 vol.% to 20 vol.% due to laser surface melting is significant. The volume fraction of β-Ti following melting is attributed to the stabilisation of acicular martensite in the structure during rapid quenching. In surface nitriding, mainly titanium nitride, 94 % is produced, with only a very small amount of α-Ti (6 %). The formation of β-Ti is fully suppressed by nitriding. From Table 1 it is also relevant that very low tensile residual (maximum up to 0.639 %) micro-strain is induced within the melted and nitrided zone of the surface treated Ti-6Al-4V samples mainly due to a very high thermal gradient developed and the related quench stress built thereafter. A detailed study concerning the effect of process parameters on the magnitude of micro-strain has been reported elsewhere [24].

Properties of the melted/nitrided layer

Micro-hardness of the top surface and cross section of the laser surface melted and laser surface nitrided Ti-6Al-4V was carefully measured to observe the influence of laser surface modification on micro-hardness and its distribution. Figure 5 shows the variation of micro-hardness with depth from the surface of laser surface melted (plot 1 and plot 2) and laser surface nitrided (plot 3 and plot 4) Ti-6Al-4V samples lased under different processing conditions. Laser surface melting was found to improve the micro-hardness of the melted region from 260 Hv of as received surface to a maximum of 490 Hv. The micro-hardness in the melted region was however, almost uniform along depth and decreased to a value of substrate micro-hardness at the solid-liquid interface. The improvement in micro-hardness of the melt zone is attributed to refinement of microstructure and formation of acicular martensite during rapid quenching. On the other hand, micro-hardness of the nitrided layer was improved to 2–3 times (to a maximum of 950 Hv) as compared to that of as-received Ti-6Al-4V. Like melting, the average micro-hardness of the nitrided layer was found to be almost uniform and gradually decreased to the substrate micro-hardness at the nitrided layer-substrate interface. Significant improvement in micro-hardness of the nitrided layer is attributed to the formation of titanium nitrides at the

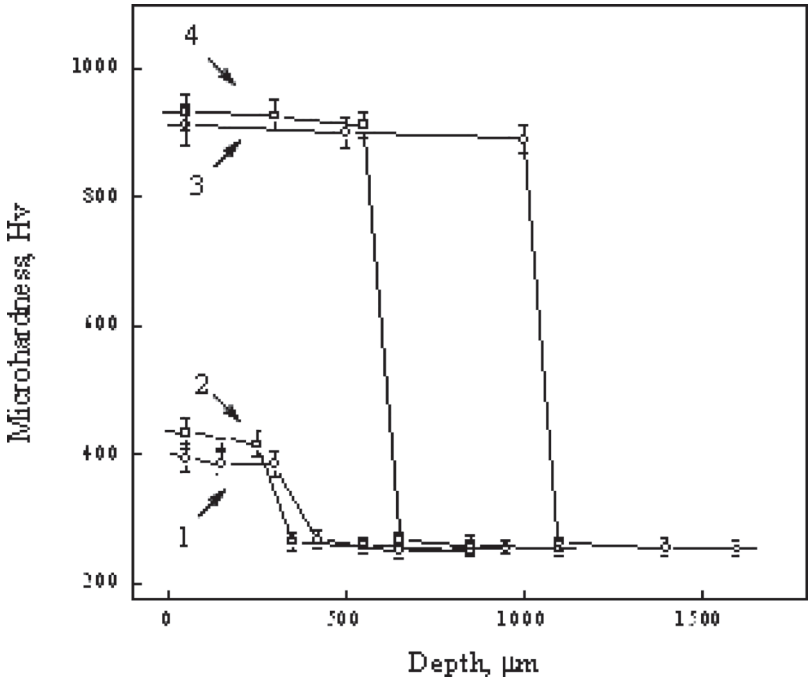

FIGURE 5
Variation of micro-hardness with depth from the surface of laser melted Ti-6Al-4V with a power of 800 W (plot 1), 600 W (plot 2) and laser nitrided Ti-6Al-4V with a power of 800 W (plot 3), 600 W (plot 4) respectively.

nitrided surface. The average micro-hardness of the melted and nitrided layer was also found to vary with laser parameters.

Figure 6 shows the potentio-dynamic cyclic polarization behaviour of as received (plot 1), laser surface melted (with a power of 700 W, plot 2) and laser surface nitrided (with a laser power of 700 W, plot 3) Ti-6Al-4V. Table 2 summarizes the corrosion parameters derived from Figure 6. A close comparison of different plots in Figure 6 shows that E_{corr} value for laser surface melted sample shifts significantly towards nobler direction. Shifting in E_{corr} for laser surface melted Ti-6Al-4V samples may be possibly attributed to formation of acicular martensite and reduction in volume

TABLE 2
Summary of the corrosion characteristics of surface melted and nitrided Ti-6Al-4V.

Sp. no.	Specimen history	Laser power (W)	E_{corr} (mV)	E_{pp1} (mV)	E_{pp2} (mV)
1	Ti-6Al-4V	As received	−259	1309	251
2	Melted Ti-6Al-4V	700	2431	5450	2900
3	Nitrided Ti-6Al-4V	700	−215	1875	125

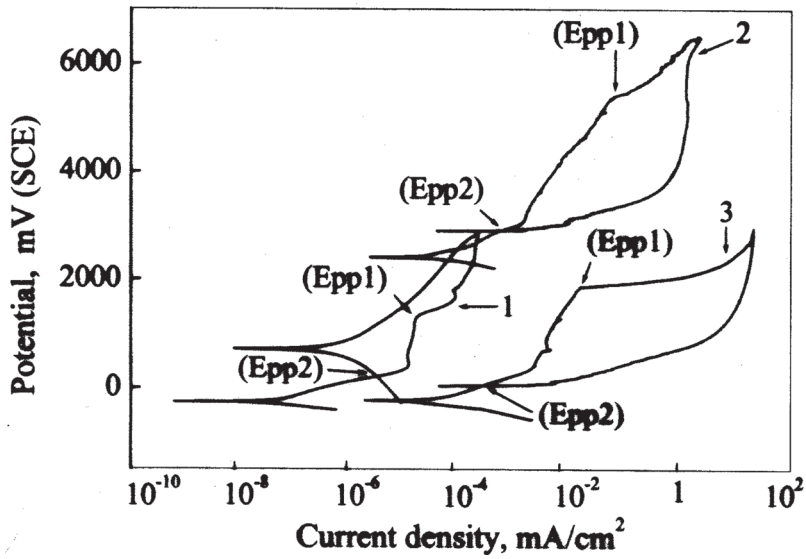

FIGURE 6
Potentiodynamic cyclic polarization behaviour of (1) as received, (2) laser surface melted (with a power of 700 W) and (3) laser surface nitrided (with a power of 700 W) Ti-6Al-4V.

fraction of β phase following laser surface melting**.** On the other hand, E_{corr} of laser surface nitrided sample is comparable to that of as-received Ti-6Al-4V samples. Similar E_{corr} level, even though absence of β-Ti in laser nitrided samples is attributed to presence of nitrides. On the other hand, critical potential for pit formation (E_{pp1}) of laser surface melted sample is significantly higher (5450 mV(SCE)) as compared to as-received Ti-6Al-4V (1309 mV(SCE)). The improved pitting corrosion property by surface melting is possibly because of partial suppression of β phase formation in the microstructure and change in morphology from granular to acicular. Hence, it may be concluded that laser surface melted Ti-6Al-4V showed a superior pitting corrosion property. When processed under similar condition (700 W), E_{pp1} value of laser surface nitrided Ti-6Al-4V is significantly decreased (to 1875 mV(SCE) as compared to 5450 mV(SCE) for laser surface melted Ti-6Al-4V substrate, though was superior to that of as-received Ti6Al4V (1309 mV(SCE)). The relatively poor pitting corrosion property of laser surface nitrided Ti-6Al-4V as compared to surface melted Ti-6Al-4V (processed under similar laser power) is because of the presence of a significantly large volume fraction of TiN in the microstructure and the interface between the TiN and α-Ti favouring the pit formation. Potential for pit growth (E_{PP2}) was however, nobler than E_{corr} of the respective samples, and hence, even though there is formation of pits its growth would be prohibited [26]. However, it is relevant to note that E_{corr}, E_{PP1} and E_{PP2}

were found to vary with laser parameters. A detailed study concerning the influence of laser parameters on the corrosion behaviour and genesis of the differential behaviour is under investigation [24].

Cell proliferation on each specimen was measure by MTT assay. The cleavage of MTT has several desirable properties for assaying cell survival and proliferation. The tetrazolium salts, such as MTT, are reduced into coloured formazan compounds by all living, metabolically active cells. The biochemical procedure is based on the activity of mitochondrial enzymes which are inactivated shortly after cell death. The main advantage of the colorimetric assay is the speed with which samples can be processed. The assay can be read a few minutes after the addition of dimethyl sulfoxide, for dissolving the non-soluble formazan compound, and the colour is stable for a few hours at room temperature. The results are also apparent visually, which is very useful if rapid qualitative results are required [36–38]. Cell attachment is expressed in terms of percentage of adhered cells with respect to the positive control (Petri plate). The results after 72 hours of cultivation are shown in Figure 7 and are summarized in Table 3. The number of cells in as received, laser surface melted and laser surface nitrated exceeds the positive control (100%). However it is observed that the percentage increase in cell number is maximum for laser surface nitrided and minimum for laser surface melted Ti-6Al-4V. In this regard, it is relevant to mention that Ti-6Al-4V is widely used for bio-implant application with an excellent bio-compatibility. The present study was aimed at improving the wear resistance of Ti-6Al-4V by surface melting and surface nitriding. By surface

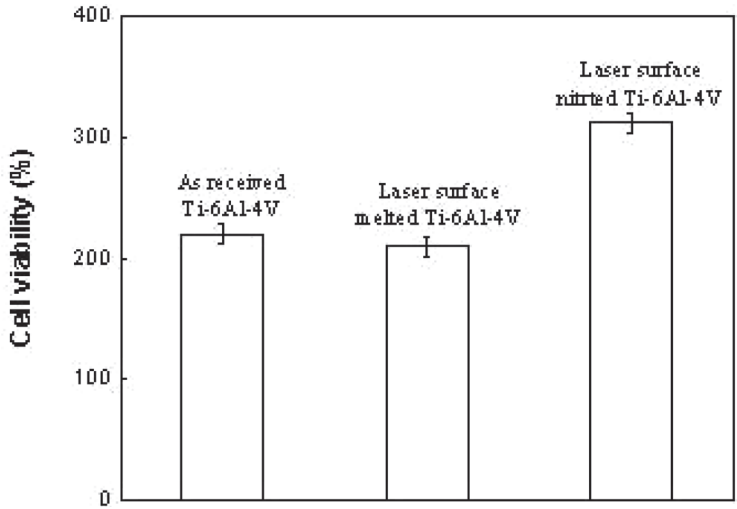

FIGURE 7
Percentage of cell viability in relation to the positive control for as received, laser surface melted and laser surface nitrided Ti-6Al-4V.

TABLE 3
Summary of the Biocompatibility Behaviour of As-received and Laser Surface Treated Ti-6Al-4V samples.

Sp. No.	Specimen	MTT reading O.D. at 595 nm	Percentage of increase in cell number
1	Control(plastic surface)	0.734	100
2	As received Ti-6Al-4V	1.614	219.8
3	Laser surface melted Ti-6Al-4V	1.274	173.5
4	Laser surface nitrided Ti-6Al-4V	2.295	312

melting though a significant improvement in wear resistance was achieved, biocompatibility is marginally deteriorated which might be attributed to partial suppression of β phase due to rapid solidification. On the other hand, surface nitriding was found to improve wear resistance with a significant improvement in bio-compatibility. In this regard, it is relevant to mention that Hao *et al*. [39] reported an improved osteoblast cell adhesion by high power diode laser treatment of Ti-6Al-4V in O_2 environment mainly due to enhanced wettability characteristics of the treated material. A detailed analysis concerning the influence of the non-equilibrium microstructure on the bio-compatibility and the genesis of improved bio-compatibility behaviour of laser nitrided surface is under investigation [24].

SUMMARY AND CONCLUSIONS

In the present study, an attempt has been made to modify the surface of Ti-6Al-4V substrate by laser surface melting and nitriding for bio-implant application. Both laser surface melting and laser surface nitriding have been carried out using a laser-line diode laser. From the results the following conclusions may be drawn:

1. Laser surface melting led to a significant refinement of microstructure and formation of acicular martensite with partial suppression of β phase. On the other hand, laser surface nitriding caused formation of TiN dendrites in α-Ti matrix.
2. Micro-hardness of the surface melted layer was improved (to a maximum of 450 Hv) as compared to 260 Hv of the as-received substrate. On the other hand, the micro-hardness in the nitrided layer was improved to 900-950 Hv. Micro-hardness was found to be uniform all throughout the melted and nitrided layer.
3. Laser surface melting was found to make the surface nobler as compared to as-received Ti-6Al-4V with a significant improvement in E_{pp1}.

4. Laser surface nitriding does not change E_{corr} significantly. However, E_{pp1} is increased as compared to as-received Ti-6Al-4V substrate.
5. Biocompatibility behaviour showed an increased number of cell viability due to surface nitriding and a marginal decrease in cell viability due to surface melting as compared to as-received Ti-6Al-4V.

ACKNOWLEDGEMENTS

The financial support for this work was provided by The Department of Science and Technology (BOYSCAST and SERC schemes), The Council of Scientific and Industrial Research (CSIR), N. Delhi and The Board of Research on Nuclear Science (BRNS), Bombay The Experimental Support from the Univ. of Manchester, T. U. of Clausthal and the IIT Kharagpur is also gratefully acknowledged.

REFERENCES

[1] Probst, J., Gbureck, U., and Thull, R. (2001). *Surf. Coat. Technol., 148,* 226.

[2] Meletis, E. I., Cooper, C. V., and Marchev, K. (1999). *Surf. Coat. Technol., 113,* 201.

[3] Fukumoto, S., Tsubakino, H., Inoue, S., Liu, L., Terasawa, M., and Mitamura, T. (1999). *Mater Sci Eng A, 263,* 205.

[4] Wang, R. R., Welsch, G. E., and Monteiro, O. (1999). *J. Biomed. Mater. Res., 46,* 262–270.

[5] Kuo, M. C., and Yen, S. K. (2002). *Mater. Sci. Eng. C, 20,* 153–160.

[6] Shi, W., Kamiya, A., Zhu, J., and Watazu, A. (2002). *Mater. Sci. Eng. A, 337,* 104–109.

[7] Thian, E. S., Khor, K. A., Loh, N. H., and Tor, S. B. (2001). *Biomaterials, 22,* 1225–1232.

[8] Lynn, A. K., and DuQuesnay, D. L. (2002). *Biomaterials, 23,* 1937–1946.

[9] Mordike, B. L. (1997). *Progress in Materials Science, 42,* 357–372.

[10] Bertoti, I., Mohai, M., Sullivan, J. L., and Saied, S. O. (1995). *Appl. Surf. Sci., 84,* 357.

[11] Man, H. C., Zhang, X. M., Yue, T. M., and Lau, W. S. (1997). *J. Mate.r Process. Technol.,66,* 123–129.

[12] Majumdar, J. Dutta, and Manna, I. (2003). *Sadhana, 28,* 495.

[13] Majumdar, J. Dutta (2000). PhD Dissertation, T. U. Clausthal, Germany, Yr.: ISBN No.: 3-89720-385-5.

[14] Mordike, B. L. (1986). Laser Surface Treatment of Metal. Draper CW and Mazzoldio P. (Eds.), Martinus Nijhoff, Dordrecht, 389.

[15] Jiang, P., He, X. L., Li, X. X., Yu, L. G., and Wang, H. M. (2000). *Surf. Coat. Technol., 130,* 24.

[16] Garcia, I., and Damborenea, J. J. D. (1998). *Corros. Sci., 40,* 1411.

[17] Bell, T., Bergmann, H. W., Lanagan, J., Morton, P. H., and Staines, A. M. (1986). *J. Surf. Engg., 2,* 133.

[18] Walker, A., Folkes, J., Steen, W. M., and West, D. R. F. (1986). *J. Surf. Engg., 1,* 133.

[19] Bell, T., Sohi, M. H., Betz, J. R., and Bloyce, A. (1990). *Scand J. Met., 19,* 218.

[20] Mridha, S., and Baker, T. N. (1994). *Mater. Sci. Engg. A, 188,* 229.

[21] Hu, C., Xin, H., Watson, L. M., Baker, T. N. (1997). *Acta Mat., 45,* 4311–4322.

[22] Robinson, J. M., Van Brussel, B. A., De Hosson, J. Th. M., and Reed, R. C. (1996). *J. Mater. Sci., 204,* 143.

[23] Man, H. C., Cui, Z. D., and Yang, X. J. (2002). *Applied Surface Science, 199,* 293–302.

[24] Biswas, A., Chatterjee, U. K., Manna, I., Li, L., and Dutta Majumdar, J. (under preparation).

[25] Cullity, B. D., and Stock, S. R. (2001). *Elements of X-Ray Diffraction* (Third Edition), 435. Prentice Hall, N. Delhi.

[26] Fontana, M. G. (1987). *Corrosion Engineering*, 71. McGraw-Hill, New York.

[27] Mosmann, T. (1983). *J. Immun. Meth., 65,* 55.

[28] Denizot, F., and Lang, R. (1986). *Journal of lmmunological Methods, 89,* 271.

[29] Ferrari, M., Fornasiero, M. C., and Isetta, A. M. (1990). *Ibi, 131,* 165.

[30] Hongo, T., Fujii, Y., and Igarashi, Y. (1990). *Cancer, 65,* 1263.

[31] Berridge, V., and Tan, A. S. (1993). *Arch Biochem Biophys, 82,* 303–474.

[32] Welding, Brazing and soldering. *ASM Handbook* (1993), Vol. 6, ASM International, Materials Park, OH.

[33] Manna, I., and Majumdar, J. Dutta (1995). *Z Metallkde, 86,* 362–364.

[34] Kloosterman, A. B., and De Hosson, J. Th. M. (1995). *Scripta Metal. Mater., 33,* 567.

[35] Murray, J. L. (1990). Phase diagrams in binary titanium alloys. ASM International, Materials Park, OH., 176.

[36] Hillmann, G., Gebert, A., and Geurtsen, W. (1999). *J. Cell Science, 112,* 2823–2832.

[37] Sjögren, G., Sletten, G., and Dahl, J. (2000). *J. Prosthet Dent., 84,* 229–36.

[38] Edmondson, J. M., Armstrong, L. S., and Martinez, A. O. (1988). *J. Tissue Culture Method, 11,* 15–17.

[39] Hao, L., Lawrence, J., and Li, L. (2005). *Applied Surface Science, 247,* 602–606.